Microbial Paper: Cellulose Fiber-based Photo-Absorber Producing Hydrogen Gas from Acetate using Dry-Stabilized *Rhodopseudomonas palustris*

Oscar I. Bernal,[a] Joel J. Pawlak,[b] and Michael C. Flickinger [c,*]

The microstructure and reactivity of a novel nonwoven cellulose fiber cellular biocomposite (microbial paper) was studied relative to long-term stabilization of potentially any microorganism. Cells were incorporated during the papermaking process as an integral component of a highly porous cellular biocomposite that can be dry stabilized. Hydrogen gas production from acetate *via* the activity of the nitrogenases in *Rhodopseudomonas palustris* CGA009, entrapped at a very high concentration, in hand-made microbial paper was sustained for > 1000 h at a rate of 4.0 ± 0.28 mmol H_2/m^2 h^{-1} following rehydration. This rate is 2x and 10x greater than previously reported H_2 production rates by *Rps. palustris* latex coatings that were dried on polyester and non-dried formulations applied to the surface of paper, respectively. By vacuum-dewatering and controlled drying steps to the microbial papermaking process and incorporating blends of microfibrillar (MFC), softwood (SW), and hardwood (HW) cellulose fibers, microbial paper films were fabricated that produced H_2 gas at 3.94 ± 1.07 mmol H^2/m^2 h^{-1} and retain up to 60 mg/m^{-2} dry cell weight (DCW) of *Rps. palustris*. The MFC content appears to determine the final cell load and may affect gas/moisture mass transfer properties of the biocomposite.

*Contact information: a: Department of Chemical and Biomolecular Engineering, North Carolina State University, 911 Partners Way Raleigh, NC 27695 USA; b: Department of Forest Biomaterials, North Carolina State University, Campus Box 8005 Raleigh, NC 27695 USA; c: Golden-LEAF Biomanufacturing Training and Education Center, North Carolina State University, 850 Oval Drive, Raleigh, NC 27695 USA; *Corresponding author: michael_flickinger@ncsu.edu*

INTRODUCTION

The ability to immobilize a high number of viable and reactive microorganisms on a surface is a simple and inexpensive approach to functionalize catalytically inert materials and intensify bioreactivity several-fold. However, if the supporting material is porous, then there is an inherent limitation associated with most cellular biocoating methods. Only the most superficial layers of the substrate are effectively utilized for immobilization of micron-sized cells, wasting most of the available internal pore space surface area. Flickinger *et al.* (2017) recently reviewed the advantages regarding biocoating productivity and effectiveness. This intrinsic drawback can be overcome by developing methods that incorporate biomass during the early stages of substrate manufacturing rather than as a finishing treatment applied superficially to a pre-made immobilization matrix. This reasoning prompted the authors to investigate the fabrication method of porous paper as a support for photosynthetic cells to adapt it for solar energy trapping and for the production of hydrogen gas.

Paper has been present in human history since its original conception in China, first recorded in 105 AD. The original fiber sources (fishnets, clothing, hemp, and mulberry bark (Hunter 1978)) have been replaced by wood-derived fibers that can be produced in different sizes and morphologies (Siro and Plackett 2010; Zhang *et al.* 2013). The method itself has evolved from using fixed-screen molds, couching (transferring wet paper sheets to felt surfaces), and screw-presses to modern paper machines capable of producing continuous paper strips at very high speeds (Hubbe and Bowden 2009).

The most recent technology development is the use of nanostructured celluloses as building blocks for the development of sustainable functional materials (Isogai and Berglund 2013). Cellulose nanofibrils (collectively called microfibrillar cellulose (MFC) or nanofibrillar cellulose (NFC)) have excellent mechanical properties, large surface areas, and a variety of surface functional groups suitable for use as targets for functionalization (Zhang *et al.* 2013). The process to obtain cellulose micro- and nanofibrils from native cellulose fibers is energy intensive, generally involving an additional refining step followed by several high-pressure homogenizations (Zimmermann *et al.* 2004). However, the resulting MFC product (microfibril aggregates, 20 to 100 nm in diameter and up to several microns long) is capable of imparting novel interesting optical, mechanical, thermal, and biological functionalities to composite materials. This includes the capability to retain high concentrations of viable microorganisms as part of the matrix while preserving viability and reactivity.

Microbial contamination is always present throughout the papermaking process and is gradually eliminated by high pressures, mechanical shear, and varying temperatures used to achieve the final mechanical strength of the material. Contaminating biofilm (slime) samples can be collected from the wet end of paper and board machines using recycled fiber or unbleached pulp. Slime commonly yields between 2.0×10^{10} to 2.6×10^{12} bacterial cells per gram (Vaisanen *et al.* 1994), and cells are usually embedded within a matrix of polysaccharides. Among these cells, aerobic bacteria are the predominant colonizers, especially members of the genus *Bacillus*, with few or no yeast and molds present (Vaisanen *et al.* 1991, 1998). In the final paperboard product, bacteria belonging to the genera *Bacillus*, *Paenibacillus*, and *Brevibacillus* are usually found in quantities from < 50 to 250 cfu g^{-1} in homogenized paperboard (Suihko and Skytta 1997; Pirttijarvi *et al.* 2000; Suihko and Stackebrandt 2003), which shows how the papermaking process drastically reduces total microbial counts. More interestingly, confocal scanning electron microscopy of coated food-grade papers has shown that most of the surviving microflora accumulates in the interface between the cellulose fibers and the coating (polyethylene, mineral pigments, or biodegradable polymer). Soluble nutrients and no antimicrobial compounds were found, which indicates that the limiting factor for bacterial proliferation in the paper was the access to free water even under conditions of extensive wetting (Suominen *et al.* 1997).

Aside from studies on the characterization of the residual microbial contamination after the papermaking process, there are very limited reports on the deliberate incorporation of live microorganisms into a pulp suspension prior to film formation. In one example, bacteria (*Bacillus cereus*) were used to produce handsheets of paper under controlled laboratory conditions (drying temperature 80 °C) as a model system to obtain risk assessment data in cellulosic fiber-based materials (Hoornstra *et al.* 2006). Under these conditions, only 5% of the vegetative cells and spores were retained in the paper.

Real time-polymerase chain reaction (RT-PCR) has been used to detect and quantify this same organism in cardboard and paper (Priha *et al.* 2004). No attempt was made to alter the papermaking process or to add protective substances to optimize the bioreactivity of the final paper. A low number of bacilli survive the traditional papermaking process when the paper is dried at 80 °C.

No functionality or reactivity has ever been added to the paper other than to show the presence of bacilli in the final product. In a related, yet extremely different approach, Liu and collaborators were able to encapsulate individual cells of *Pseudomonas*, *Zymomonas*, and *Escherichia* in individual triblock polymer fibers that remain viable for months and can efficiently exchange nutrients and metabolic products with the environment (Liu *et al.* 2009). Here, physical entrapment of the cells is achieved by electrospining a suspension of the polymer + cells, yielding a low number of bacteria actually entrapped in the fibers in a lengthy and hard-to-scale process.

Purple non-sulfur bacteria (PNSB) are a very versatile group of photosynthetic prokaryote microorganisms. These bacteria are capable of catalyzing hydrogen production under anaerobic conditions using nitrogenase with no need to protect their photosynthetic apparatus from inactivation from oxygen. In addition, they are capable of fixing atmospheric nitrogen *via* nitrogenase activity in the process (Rey *et al*. 2007). These PNSB are easily isolated from soil and water and they can grow as aerobes if oxygen is present to generate energy by respiration or as photoautotrophic organisms in the presence of light (they synthesize the light absorbing pigments and they acquire a characteristic color depending on the species) with the production of H_2 by cyclic photophosphorylation (Harwood 2008).

Over 20 genera of PNSB have been described, but most of the current knowledge about the group comes from studies on four species: *Rhodospirillum rubrum*, *Rhodobacter capsulatus*, *Rhodobacter sphaeroides*, and *Rhodopseudomonas palustris*, the latter being the most interesting given its extraordinary robustness and the presence of the genes that encode all three nitrogenase isozymes in its genome (Oh *et al.* 2004; Kars and Gunduz 2010). These characteristics also make them convenient model organisms for studies on cellular immobilization (Gosse *et al.* 2007, 2010, 2012), photobioreactor design and illumination optimization (Adessi and De Philippis 2014), and pigment content manipulation at the molecular level (Ma *et al.* 2012) to improve H_2 production yields under anoxic conditions. Immobilized systems including PNSBs are an integral component of the current efforts to bring microbial hydrogen production to the marketplace (Show *et al*. 2012).

Additional applications of microbial papers beyond solar energy generation include: reactive filters that can act both as support for reactive cells (capable of performing complex biotransformations) and as a filter to separate the products from substrate material, bioremediation supports, biodegradable disposable biosensors and smart structural materials (fiberboard) for construction and packaging applications. The microbial paper manufacture methods described in this paper are novel, simple, and inexpensive, and conceptually compatible with the current papermaking infrastructure in place (suggesting scalability).

The authors report proof of concept reactivity and microstructure data that will open the path for a new generation of sustainable cellular biocomposite materials for diverse applications in biomanufacturing.

EXPERIMENTAL

Materials

Bacterial strain, media, and growth conditions

Rhodopseudomonas palustris wild type CGA009 was grown anaerobically in 160-mL glass serum bottles (Wheaton, Millville, NJ) containing 100 mL of a nitrogen fixing photosynthetic medium PM(NF) (Rey *et al*. 2006) with an initial headspace pressure of 1 atm N_2. Cultures were incubated at 30 °C under 35 PAR µmol photons m^{-2} s^{-1} (LI-COR, LI-190SA Quantum Sensor, Lincoln, NE) 40 cm below two 60-W clear incandescent lights without shaking.

The PM(NF) was composed of (per liter): 25 mL of 0.5 M Na_2HPO_4, 25 mL of 0.5 M KH_2PO_4, 1 mL of 0.1 M sodium thiosulfate, 1 mL of 2 mg/mL para-aminobenzoic acid, 20 mL of 1 M sodium acetate, and 1 mL of concentrated base solution. The concentrated base solution was composed of (per liter): 20 g of nitrilotriacetic acid, 28.9 g of $MgSO_4$, 6.67 g of $CaCl_2 \cdot H_2O$, 18.5 mg of $(NH_4)_6Mo_7O_{24} \cdot 7H_2O$, 198 mg of $FeSO_4 \cdot 7H_2O$, and 100 mL of metal 44 solution.

The metal 44 solution was composed of (per liter): 2.5 g of ethylene diamine tetra-acetic acid (EDTA) (free acid), 10.95 g of $ZnSO_4 \cdot 7H_2O$, 5.0 g of $FeSO_4 \cdot 7H_2O$, 1.54 of $MnSO_4 \cdot H_2O$, 392 mg of $CuSO_4 \cdot 5H_2O$, 250 mg of $Co(NO_3)_2 \cdot 6H_2O$, and 177 mg of $Na_2B_4O_7 \cdot 10H_2O$.

Hand-made microbial paper: Proof of concept method

Paper pulp was prepared by the disintegration and blending of two regular bleached copy paper sheets (Domtar, Fort Mill, South Carolina) in 500 mL of diH_2O for a final solids concentration of 2% solids, using a household blender (Oster, Boca Raton, FL) at maximum speed. This paper pulp was mixed with 100 mL of an optical density (OD) 540 ≈ 3, 7-day-old *Rps. palustris* culture using three different methods: simultaneous pulping and biomass mixing *via* maximum-speed blending, mixing at medium speed post-pulping, and manual mixing with a glass agitator post-pulping. The resulting bacteria/pulp suspension was left undisturbed for 15 min prior to wet lay formation to allow for incorporation of the biomass into the fiber matrix. The *Rps. palustris* microbial paper sheets were manufactured for the first time using a commercial papermaking kit (Greg Markim Inc., Milwaukee, WI). A 5.5 in x 8.5 in hardwood frame was set on a collection tray along with a mesh screen (Fig. 1). The bacteria/pulp suspension was dispensed on top of the screen and distributed manually to cover the whole mesh area. Another mesh screen was put on top of the suspension along with a hard plastic cover screen sandwiching the suspension in between. The whole set-up was tilted approximately 60° with respect to the tray while gently pushing on the edges and center of the plastic screen to eliminate water from the fiber suspension.

After no bulk water flow was observed coming from the edges of the tray, the wet paper mat (still sandwiched between the two papermaking mesh screens) was taken out of the tray and set flat on top of paper towels. Additional paper towels were set on top of the sheet and body-weight pressure was applied using a press bar horizontally, vertically, and diagonally. Finally, the two mesh screens were carefully peeled from the wet paper sheet, which was set flat on aluminum foil in an environmentally controlled chamber set at 30 °C and 60% relative humidity (RH). The paper sheet was dried overnight at these conditions.

Methods

Microbial paper film manufacturing: Vacuum dewatering method

The vacuum dewatering method allowed for more precise control over the final fiber composition, the thickness, and grammage of the microbial paper sheets (Fig. 1).
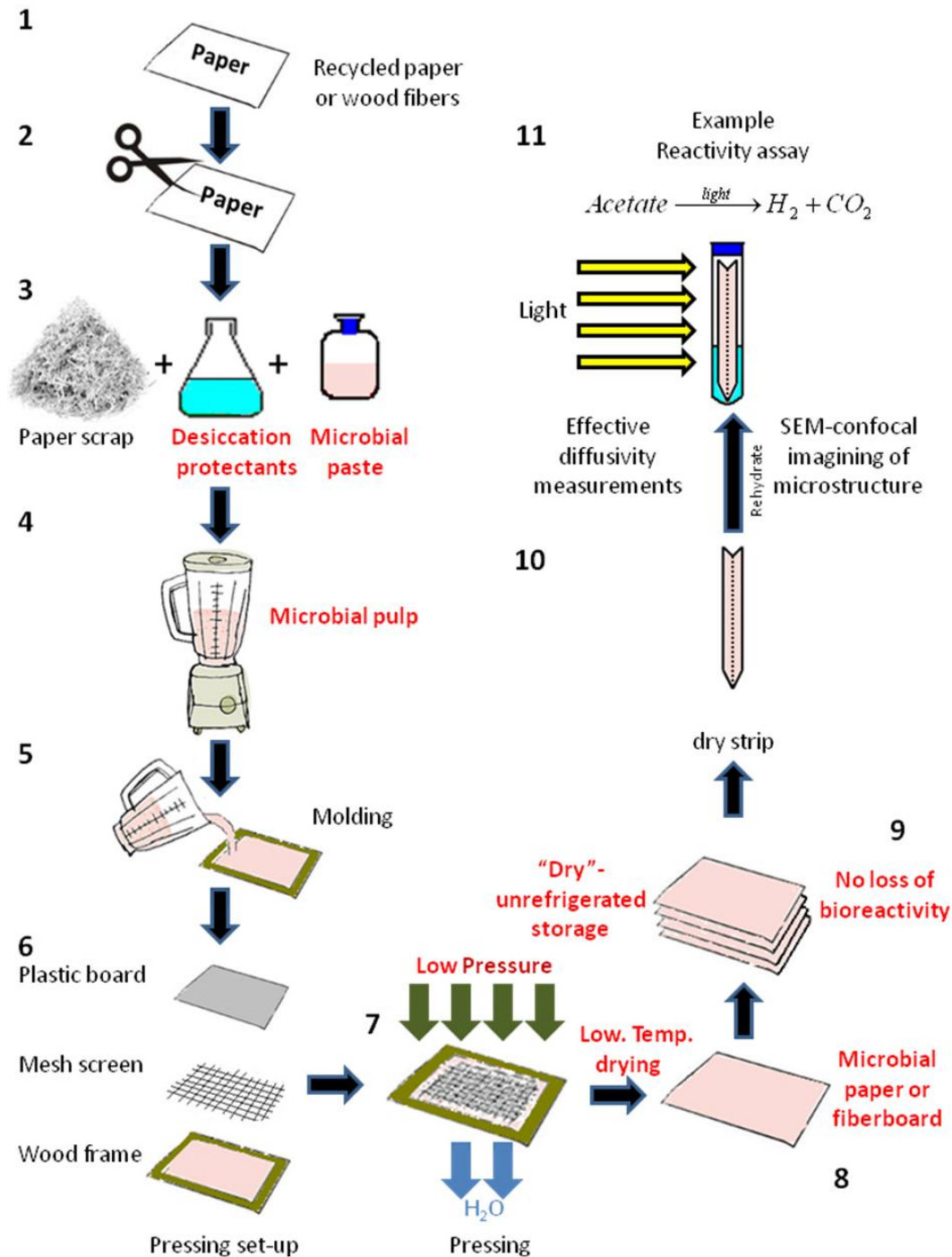
Fig. 1. Method for the fabrication of hand-made sheets of *Rps. palustris* microbial paper. The numbers indicate the stages for small-scale microbial paper manufacture and their reactivity characterization.

Paper pulps were prepared by hand-tearing bleached kraft softwood (SW) and hardwood (HW) pulp sheets into approximately 2-in squares. They were disintegrated in a standard 2-L disintegrator at 1.2% solids concentration at 3000 rpm for 5 min (TAPPI Method T-205 sp-95 1995). The final solids concentration was adjusted to 0.1% prior to storage at 4 °C. The MFC samples were produced from bleached hardwood market pulp using a 10 in disk diameter Masuko Super Masscolloider (Masuko Sangyo Co., Kawaguchi-City, Japan). The samples were processed at a 3% consistency, with no pretreatment, for 7 passes (an energy consumption of approximately 4,355 kJ/kg). The MFC diameters ranged from approximately 45 to 80 nm.

Pulp blends of these three fiber types were prepared by manually mixing the 0.1% pulp slurries in a glass beaker along with 100 mL of the *Rps. palustris* culture. Microbial paper films were manufactured by vacuum dewatering followed by restrain-drying. The pulp blend/bacterial slurries were vigorously mixed to ensure proper fibril dispersion and cellular incorporation into the fiber matrix. A Büchner funnel with an 11-cm-diameter Whatman 41 filter and a metallic mesh screen was assembled on a vacuum apparatus. The filter paper was then wetted and vacuum-sealed to the mouth of the funnel. Next, the pulp/bacteria slurry was poured into the funnel (making sure it remained leveled at all times), and the vacuum was reapplied until no bulk water flow was observed coming out of the funnel discharge. At this point, the vacuum was removed and the film-filter assemblies were removed from the funnel. Films were restrained dried still attached to the filter paper between plastic rings overnight at 30 °C and 60% RH in an incubator. The final films were ~60 g/m^2 and 50 to 100 µm thick. Samples of the original *Rps. palustris* cell pool and filtrates were collected for determination of the dry cell weight retained in the microbial paper sheets by overnight drying in an oven at 70 °C.

Determination of Headspace H$_2$ Production

The microbial paper films were cut into 2 cm x 5 cm strips and placed into vertical Balch tubes containing 10 mL of the PM(NF) medium; the tubes were sealed and flushed for 5 min with 100% Argon. All of the tubes were then vented using a water trap back to 1 atm. All films were incubated under cool fluorescent light with 100 µmol photons m^{-2} s^{-1} illumination without shaking at 25 °C. The production rates were determined by averaging over the first ~600 h of hydrogen production and reported as a single mean value.

Headspace Gas Analysis

An Agilent 7890 gas chromatograph (Santa Clara, California, USA) containing a Supelco 6' x 1/8" ID 60/80 mole sieve 5A porous mesh polymer packed stainless steel column and a thermal conductivity detector was used for headspace analysis of H$_2$, O$_2$, N$_2$, and CO$_2$. Argon was used as the carrier gas at a flow rate of 39 mL/min with injector/oven/detector temperature settings of 160°/160°/250 °C, respectively.

Material Imaging and Microstructure

Film microstructure was studied by scanning electron microscopy (SEM) using a Hitachi 3200-N Variable Pressure Scanning Electron Microscope (Chiyoda, Tokyo, Tokyo, Japan) equipped with a 4Pi Isis EDS system for digital image acquisition. All papers were observed in two or more randomized locations using a 5-kV accelerating voltage. Each location was imaged multiple times using sequential magnifications ranging from 100x to 10,000x to characterize surface topography, cell distribution, and available

pore space. Samples were sputter coated (Hummer II, Technics, Union City, California, USA) prior to imaging with a thin layer of gold in a mild vacuum (~100 mTorr of Ar gas pressure; 600 V accelerating voltage) for 5 min and immediately placed in the SEM vacuum chamber for analysis. Cross-sectional images were obtained by freeze-drying papers in liquid nitrogen and manually cryo-fracturing with a frozen sharp blade while submerged in the liquid nitrogen. These samples were mounted in a cross-sectional sample holder and sputter-coated with gold using the procedure previously described.

RESULTS AND DISCUSSION

Reactivity and Microstructure Data

The proof of concept data presented suggested successful preservation of *Rps. palustris* photoreactivity post-immobilization in the microbial paper sheet (Fig. 2A). By controlling the pressing and drying conditions the authors were able to transfer their expertise on the preservation of cellular viability in latex coatings (Gosse *et al.* 2012; Bernal *et al*. 2014; Estrada *et al.* 2015) to the fabrication of this paper-based cellular biocomposite. It was also evident from the H_2 production data that the manufacturing conditions played a critical role on the final reactivity of the microbial paper sheet. The amount of shear stress that the cells were exposed to during the biomass incorporation step seemed to affect the final photoreactivity of the paper, which was observed as substantial differences between the primary and secondary H_2 production rates *via* sheets prepared using different blending regimes. The characteristic high-shear conditions present during pulping seemed to be incompatible with long-term sustained photoreactivity, as evidenced by the early plateaus observed in sheets prepared by simultaneous pulping and blending of the biomass. The maximum H_2 production rate recorded from this first set of microbial paper sheets was 4.00 ± 0.28 mmol $H_2/$ m^{-2} h^{-1} yielding a light conversion efficiency (LCE: energy stored as hydrogen produced per unit of light energy absorbed) of 0.9%. This LCE value is comparable to that of *Rps. faecalis* cells immobilized on activated carbon fibers and slightly lower compared to *Rps. palustris* immobilized in a latex matrix (Adessi and De Philippis 2014). The H_2 production rate reported above corresponds to post-pulping manual mixing of the biomass with the suspended fibers under low-shear conditions. This rate doubles the H_2 production rate *via* latex coatings of *Rps. palustris* on polyester (Gosse *et al.* 2010) (2.08 ± 0.01 mmol $H_2/$m^{-2} h^{-1}) and is almost 10 times greater than the rate from paper coatings (Gosse *et al.* 2012) of the same organism (0.47 ± 0.04 mmol $H_2/$m^{-2} h^{-1}) previously reported by the authors. This performance is remarkable, considering that this material has not been optimized for photoreactivity, no osmoprotectants were included as part of the pulp formulation, and the papermaking method is very rudimentary.

Close inspection of hydrated *Rps. palustris* strips in the photobioreactors revealed evidence of self-tuning capabilities in response to light and nutrient availability (Fig. 2B). The pigment concentration in the headspace portion of the microbial paper strip appeared to be higher than in the submerged portion, where acetate concentration and light scattering (due to the bulk liquid phase) were higher, such that most of the metabolic activity was involved in consuming the primary carbon source. In the headspace, *Rps. palustris* cells were forced to synthesize additional photosynthetic pigment units to avoid photosaturation caused by a more direct exposure to light irradiation. Such synthesis also optimizes the use

of the limited carbon supply available in the liquid wicked from the bottom of the tube *via* capillary action.
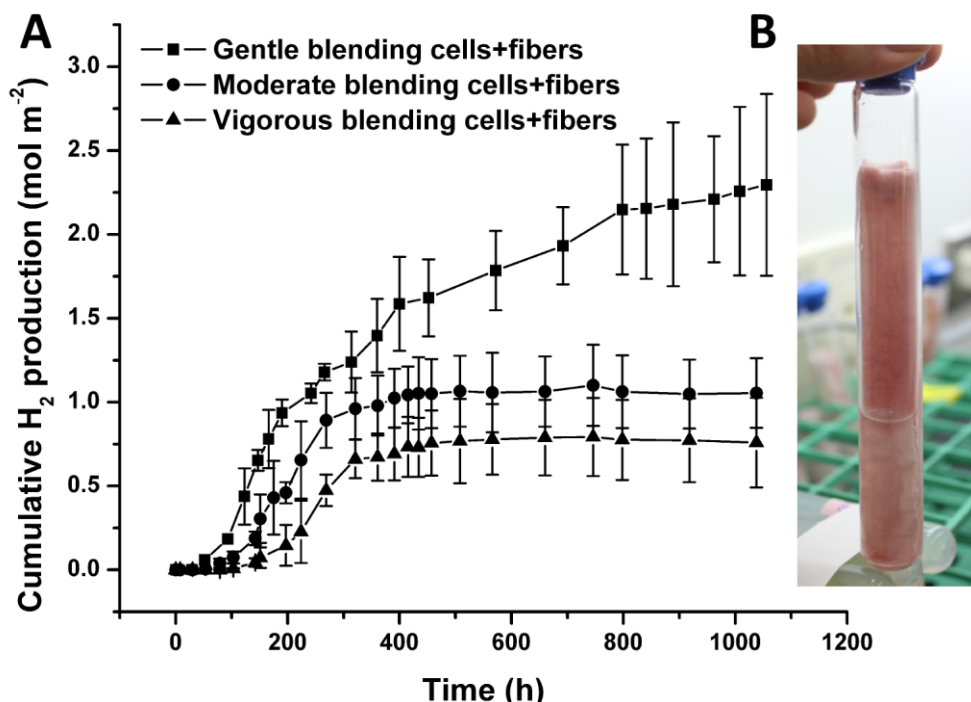
Fig. 2. Microbial paper photoreactivity: A) Long-term cumulative H_2 production by hand-made *Rps. palustris* microbial paper sheets (Error bars $\pm$ 1 Std Dev, *n* =3); and B) detail of a small-scale photobioreactor with a *Rps. palustris* paper strip at *t* = 400 h

The microstructure of the initial proof of concept microbial paper sheets provided further insight about the reasons for the high photoreactivity of this cellular biocomposite and suggested potential opportunities for improvement. The top-view SEM images of *Rps. palustris* microbial paper (Fig. 3A) revealed the distribution of the bacterial cells as clusters between paper fibers (in their characteristic rosette morphology) that did not clog the nonwoven pore space. This allowed a perfusive flow through the fiber matrix.

The cross-sectional pictures showed that bacterial cells between fibers filled the gaps and significant pore space was visible for product and nutrient transport (Fig. 3B). This structure provided a nonwoven microenvironment for cells to survive dehydration and remain viable and reactive for long periods of time after rehydration. However, the specific cellular mechanisms of dehydration survival and the mechanisms of adhesion between cells and nonwoven fibers were unknown at this point. The micrographs also revealed the presence of a wide distribution of cellulose fibers' lengths and thicknesses, which is typical for natural wood fibers used to form this paper. A precise distribution of different types of fibers would determine the final mechanical strength, mass-transfer capabilities, optical clarity, and bacterial load of the microbial paper sheet, which makes further improvement of the pulping process critical. It was also worth noting that the copy bond paper used to form this proof of concept material also contained substantial amounts of filler (calcium carbonate), salts, cationic polymers, and other additives that make copy bond paper functional.
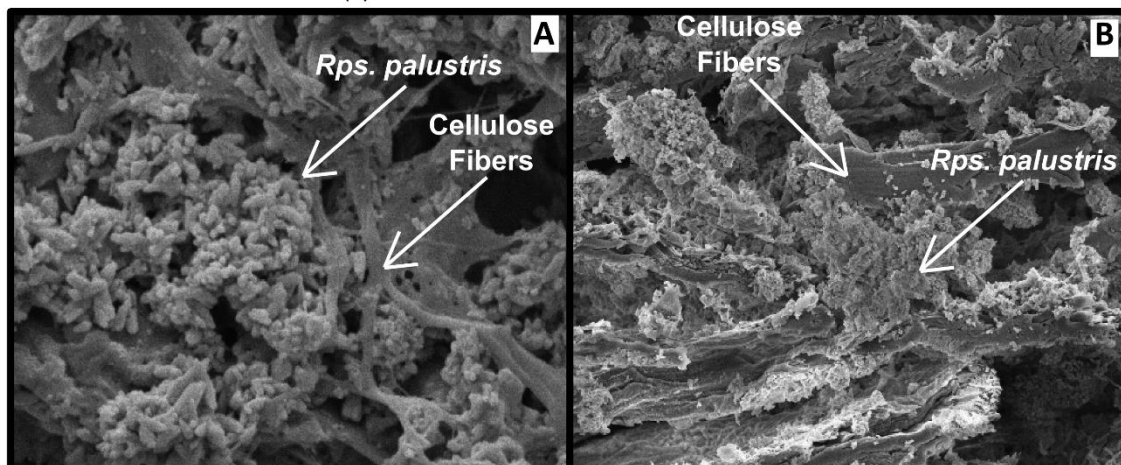
Fig. 3. Microbial paper microstructure: A) top-view SEM micrograph of a hand-made *Rps. palustris* microbial paper sheet (scale bar 2 μm); and B) cross-section (scale bar 10 μm)

Vacuum-Dewatered Microbial Paper Films

The introduction of MFC in the pulp formulation affects the final cell retention in the microbial paper film. A series of films with MFC content that ranged from 0% to 100% blended with equal parts of SW and HW fibers was prepared to characterize the effect of microfibrillar cellulose on reactivity. Filtrate samples from the vacuum dewatering process were obtained to quantify cell retention with respect to the original bacterial pool.

A qualitative inspection of the film-filtrate series (Fig. 4A) revealed a positive correlation between the MFC content and the retention of *Rps. palustris* in the film. This was evidenced by the increased intensity of the pigmentation in the film and the corresponding decreased intensity of the color in the filtrate. The specific H_2 production data revealed some unexpected trends between the MFC content and the photoreactivity of the film (Figs. 4B, C). Films in the lower MFC range had the highest specific H_2 production rates but lost specific reactivity as the MFC content increased. Given that bacterial retention in the film increased almost proportionally with MFC content, this specific reactivity drop might have been related to the mass transfer limitations as the films gained barrier properties in the upper MFC range. It is well known that pure MFC films have poor moisture diffusion coefficients and gas permeabilities (Siqueira *et al*. 2010; Lavoine *et al*. 2012), primarily as a consequence of the highly hydrogen-bonded MFC network and strong interactions with the other components of the films. The specific reactivity decrease may also be a consequence of reduced light availability to the cells in the deeper layers of the biocomposite as the biomass concentration on the surface increases (a self-shading effect). Recent studies on *Rps. palustris* (Muzziotti *et al.* 2016) have shown a positive correlation between hydrogen production and light availability as a means to dissipate the excess of reducing power produced under high light intensity conditions.

Further insight into the mass-transfer limitation problem of these blends can be provided by plotting the H_2 productivity data as a function of the film area (Figs. 5 A, B). The trend took a bell shape with a maximum cumulative production rate of 3.94 ± 1.09 mmol $H_2/m^{-2} h^{-1}$ (LCE = 1.2%) with approximately 60% MFC content. This number is still comparable to the rate observed in films made with the classical hand-made papermaking method described in the previous section. However, the physical characteristics of the vacuum-dewatered films could be more easily tuned using this improved method.
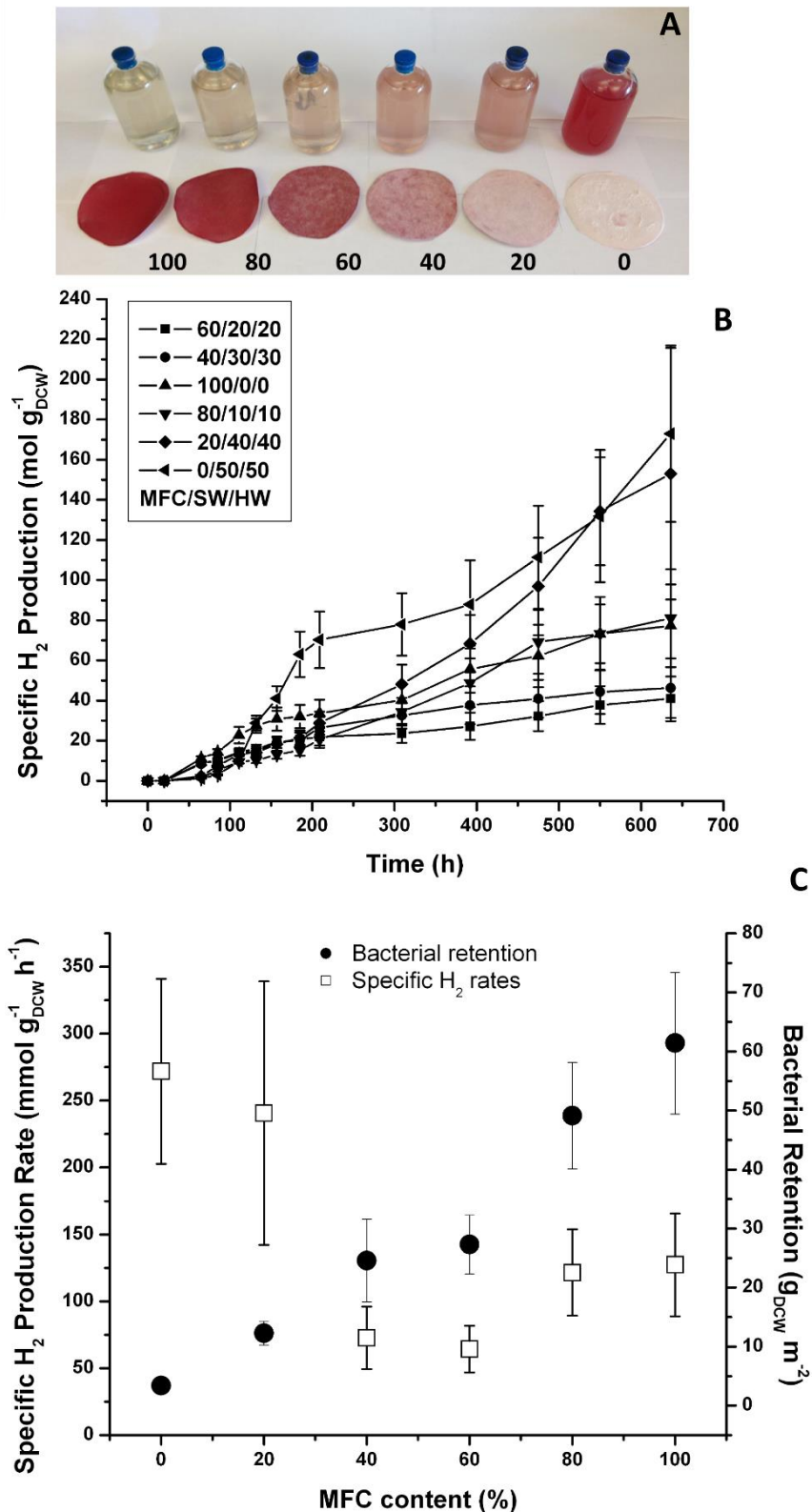
Fig. 4. Vacuum-dewatered microbial paper films specific photoreactivity: A) film/filtrate MFC series (numbers indicate MFC content (%) The filtrate is displayed with the corresponding film; B) cumulative specific H_2 production; and C) specific H_2 production rates and bacterial retention (Error bars ± 1 Std Dev, n=3)
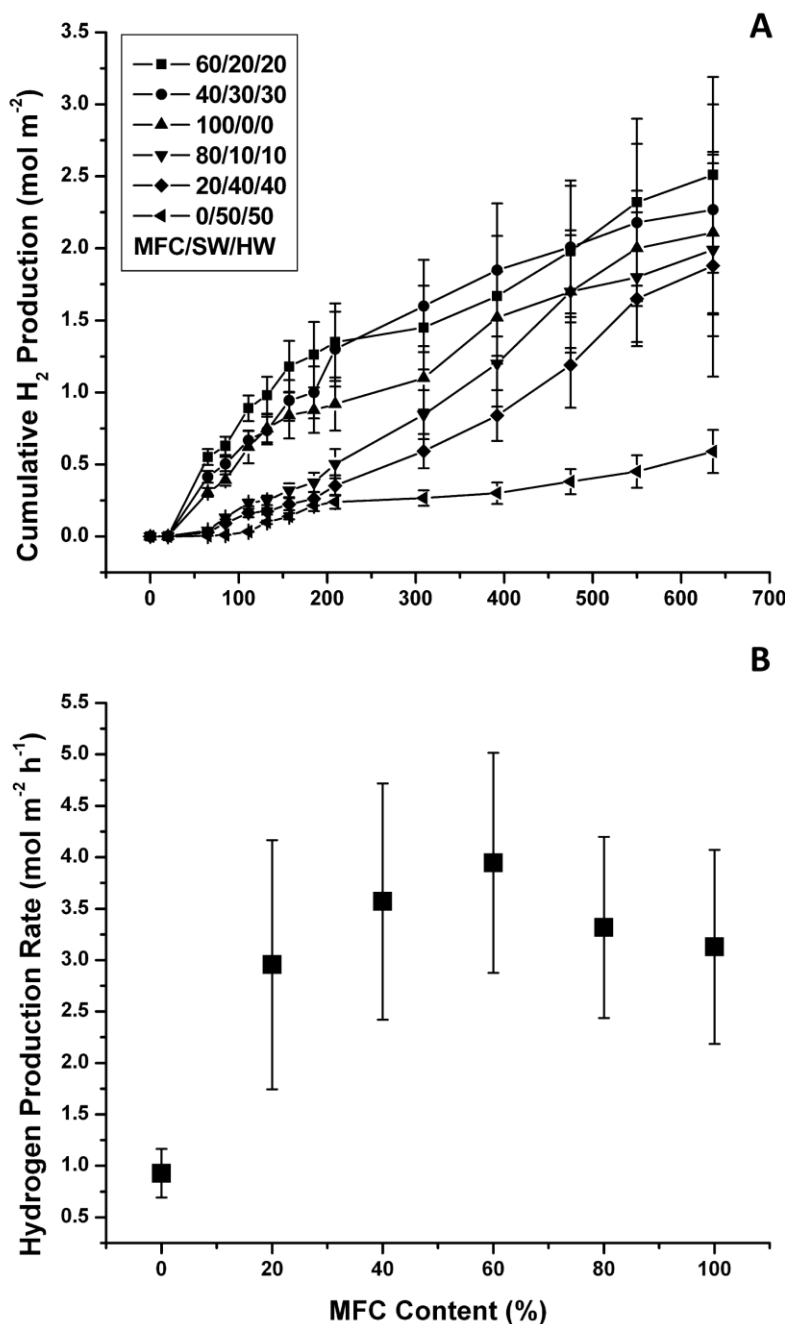
Fig. 5. Vacuum-dewatered microbial paper films photoreactivity: A) cumulative H_2 production; and B) cumulative H_2 production rates (Error bars $\pm$ 1 Std Dev, n=3)

The data also show that the H_2 production rate per m^2 decreased rapidly as the MFC content was reduced, and it was noticeably reduced in the high MFC range. At low MFC contents, the amount of retained biomass was minimal but mass transfer limitations may have been reduced, which explained the high specific H_2 productivity rates (cells are not limited by mass transfer) but rather low overall photoreactivity per m^2. In contrast, as the MFC content approached 100%, many more cells were retained, which may have resulted in reduced mass transfer that explained the low specific H_2 production rates and relatively

high photoreactivity per m^2. In this case the effect of the lower productivity per cell was counter-balanced by the presence of many more biocatalytic units per unit area.

The previous findings implied that there was a delicate trade-off between the higher bacterial retention level at high MFC contents and the observable microporosity created by the presence of thicker SW and HW fibers in the biocomposite. Top-view SEM imaging of the *Rps. palustris* films confirmed the microstructure changes that took place as the MFC content was varied (Figs. 6A, C, E, G, I, and K). Micrographs of the films show nearly continuous MFC networks at the higher MFC content with very little (if any) distinguishable microporosity. Individual *Rps. palustris* cells were visible on the surface of the film, but most of the cells appeared to be entrapped in the dense MFC matrix or entangled between the SW and HW fibers as the MFC content decreased. As the MFC content was reduced the structure "opened" and the macropore size increased, as evidenced in the cross-sectional micrographs (Figs. 6B, D, F, H, and L). Additional internal space for the perfusive flow was created by the presence of the SW and HW fibers, which further explained the higher specific H_2 productivity as the MFC content decreased.

McKinlay *et al.* (2014) recently described the effect of cellular immobilization at the metabolic level. They reported a mechanism that explains the noticeably higher H_2 yield of non-growing N_2-starved cultures of *Rhodopseudomonas palustris*. By using a combination of global transcriptome and biomass composition analysis along with ^{13}C labeled acetate tracking, they discovered non-growing cells shift their metabolism to use the tricarboxylic acid cycle to more efficiently metabolize acetate and generate more reducing power for hydrogen production. While this effect occurs, the growing cells use the glyoxylate cycle, exclusively. This recent discovery leads towards the future capability to engineer "self-tuning" mechanisms of metabolism. This is in response to nutrient limitation in cells used as non-growing biocatalysts to dramatically increase the efficiency of the incorporation of a carbon source into the product, and minimize other biosynthetic processes related to cell growth. It is also an example of how transcriptome data, alone, are not sufficient to accurately predict the observed cellular physiology to nutrient starvation, which resulted in a 3.5-fold higher hydrogen evolution rate compared to growing the *Rps. palustris* cells. The specific photoreactivity data under non-growth conditions presented in this paper is a representation of bioprocess intensification *via* cellular concentration in a highly tunable immobilization matrix. It also represents the bulk cumulative effect of metabolic self-tuning, engineered spatial distribution of biocatalytic units and optimized light and mass transfer capabilities in the microbial paper film. This cumulative effect can also be observed by direct comparison of the maximum hydrogen production rates obtained from *Rps. palustris* biocomposites fabricated by different deposition methods (Table 1).

The microbial paper concept is still an early-stage technology with many potential opportunities for improvement. The data presented in this paper are merely exploratory, but they should serve as a proof of concept foundation to continue the development of this promising concept. For example, the authors' current pulp formulation included native cellulose fibers that have not been surface-modified to better complement the surface charge of the bacterial cells. Previous literature reported methods for the chemical generation of positive charges on the cellulose microfibrils' surface (Stenstad *et al.* 2008) that could create an electrostatic interaction between the bacterial surface and the fibers.

MFC/SW/HW (%)

100/0/0   80/10/10   60/20/20

40/30/30   20/40/40   0/50/50
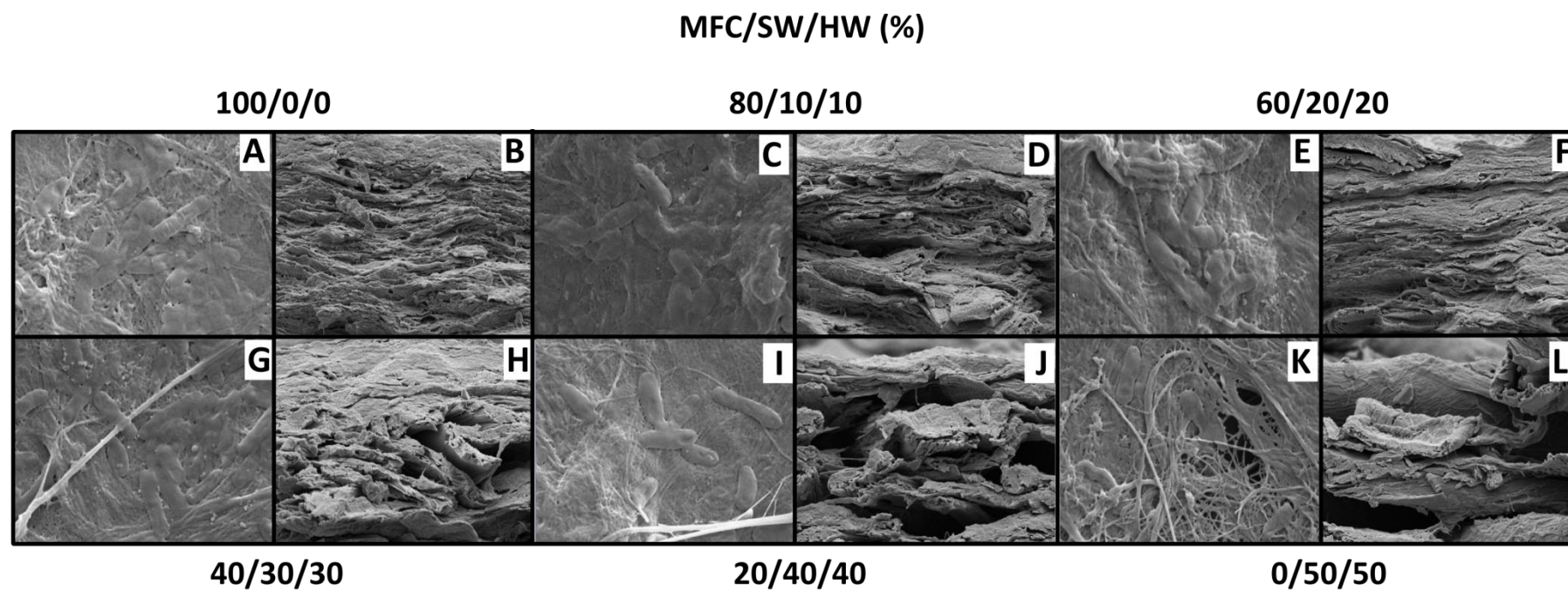
Fig. 6. Vacuum-dewatered microbial paper films: A, C, E, G, I, K: top views (scale bar 2µm); B, D, F, H, J, L: cross sections (scale bar 10µm)

bioresources.com

Table 1. Maximum H_2 Production Rates for Different *Rps. palustris* Photoreactive Materials

Material Type	Max. H_2 Production Rate (mmol H_2/ $m^{-2} h^{-1}$)	Time Elapsed at Max. H_2 Rate (h)	Reference
Paper Biocomposite	4.00 ± 0.28	600	This work
Polyester Coating	6.30 ± 0.53	120	Gosse *et al.* (2007)
Polyester Coating	2.08 ± 0.01	4000	Gosse *et al.* (2010)
Paper Coating	0.47 ± 0.04	120	Gosse *et al.* (2012)

Such a surface modification process could improve cell retention in microbial papers with a low MFC content and more desirable mass transfer properties. In the search for these optimized cell-fiber interactions, extensive characterization of the microbial papers will be necessary to find a suitable tradeoff between optical clarity/reactivity/ stability, mechanical strength, porosity, and bacterial load. The pulp and paper industry already has methods that should facilitate the adaptation of this technology to the current papermaking infrastructure.

Microbial papers and cellular composite materials are a new "smart material" technology platform that offers many potential applications. No fiber-based material with the capabilities described in this paper currently exists in the market. The markets for specialty nonwovens and specialty papers continue to expand. This potentially entirely new platform technology will add previously unimaginable functionality to papers, fiberboard, and nonwoven materials and create new opportunities in the market. There are coatings and inks that contain enzymes, biocides, or other photoreactive biomolecules, and microcrystalline cellulose. However, these "smart" biomaterials are not capable of photosynthesis, biosynthesis, or absorption of gasses or the mineralization of toxic air or water contaminants. Only intact cells have these functions in the context of a biomimetic matrix built around the cells and that are custom-tailored to intensify their reactivity.

CONCLUSIONS

1. The microbial paper concept may appear a simple approach to incorporating a high concentration of engineered microbes into paper. However, the combination of custom-tailored pulp blends and careful modification of the paper drying process resulted in a dry cellular nonwoven cellular biocomposite material that stabilized and entrapped a very high concentration of *Rps. palustris* cells.

2. The results suggest that these cells regain biological activity following rehydration and produce H_2 gas without outgrowth for hundreds to thousands of hours at rates that are already several-fold superior, compared with those of other cellular biocomposites and coatings developed in the lab. This shows the great potential of such promising technology.

3. The authors' data also show the functional and structural complexity of the cellular biocomposite that was produced: they explored the effect of some manufacturing

conditions and raw material formulations obtaining a wide range of photoreactivities, cell retention, and microstructures. Further optimization of this biomaterial and implementation at industrial scale will require an interdisciplinary approach by forest biomaterials science, microbiology, and chemical engineering. However, if microbes can be stabilized in a dry form (without needing refrigerated storage or shipping), the potential market opportunities for using cells as green catalysts is potentially very large.

4. A new model in which the biocomposite manufacture site can be separated from the site of biocomposite use might be feasible due to the availability of a highly reactive cellular biocomposite right "off the shelf." Nonwoven microbial papers have this functionality. No industry has concentrated and preserved living cells using this dry nonwovens approach. This platform technology will be the prototype of a new generation of inexpensive biocatalyst-on-a-sheet materials, where "libraries" of microbial paper sheets could be stored dry and readily available for being shipped and rehydrated on site and used for a myriad of biomanufacturing, environmental, and bioenergy applications.

REFERENCES CITED

Adessi, A., and De Philippis, R. (2014). "Photobioreactor design and illumination systems for H_2 production with anoxygenic photosynthetic bacteria: A review," *International Journal of Hydrogen Energy* 39(7), 3127-3141. DOI: 10.1016/j.ijhydene.2013.12.084

Bernal, O. I., Mooney, C. B., and Flickinger, M. C. (2014). "Specific photosynthetic rate enhancement by cyanobacteria coated onto paper enables engineering of highly reactive cellular biocomposite leaves," *Biotechnology Bioengineering* 111(10), 1993-2008. DOI: 10.1002/bit.25280

Estrada, J. M., Bernal, O. I., Flickinger, M. C., Muñoz, R., and Deshusses, M. A. (2015). "Biocatalytic coatings for air pollution control: A proof of concept study on VOC biodegradation," *Biotechnology Bioengineering* 112(2), 263-271. DOI: 10.1002/bit.25353

Flickinger, M. C., Bernal, O. I., Schulte, M. J., Broglie, J. J., Duran, C. J., Wallace, A., Mooney, CharlesC. B. and Velev, OrlinO. D. (2017). "Biocoatings: Challenges to expanding the functionality of waterborne latex coatings by incorporating

concentrated living microorganisms," *Journal of Coatings Technology and Research*, In Press. DOI: 10.1007/s11998-017-9933-6

Gosse, J. L., Chinn, M. S., Grunden, A. M., Bernal, O. I., Jenkins, J. S., Yeager, C., Kosourov, S., Seibert, M., and Flickinger, M. C. (2012). "A versatile method for preparation of hydrated microbial-latex biocatalytic coatings for gas absorption and gas evolution," *Journal of Industrial Microbiology & Biotechnology* 39(9), 1269-1278. DOI: 10.1007/s10295-012-1135-8

Gosse, J. L., Engel, B. J., Hui, J. C., Harwood, C. S., and Flickinger, M. C. (2010). "Progress toward a biomimetic leaf: 4,000 H of hydrogen production by coating-stabilized nongrowing photosynthetic *Rhodopseudomonas palustris*," *Biotechnology Progress* 26(4), 907-918. DOI: 10.1002/btpr.406

Gosse, J. L., Engel, B. J., Rey, F. E., Harwood, C. S., Scriven, L. E., and Flickinger, M. C. (2007). "Hydrogen production by photoreactive nanoporous latex coatings of nongrowing *Rhodopseudomonas palustris* CGA009," *Biotechnology Progress* 23(1), 124-130. DOI: 10.1021/bp060254

Harwood, C. S. (2008). "Nitrogenase-catalyzed hydrogen production by purple nonsulfur photosynthetic bacteria," in: *Bioenergy*, J. D. Wall, C. S. Harwood, A. Demain (eds.), ASM Press, Washington, pp. 259-271.

Hoornstra, D., Dahlman, O., Jaeaeskelaeinen, E., Andersson, M. A., Weber, A., Aurela, B., Lindell, H., and Salkinoja-Salonen, M. S. (2006). "Retention of *Bacillus cereus* and its toxin, cereulide, in cellulosic fibres," *Holzforschung* 60(6), 648-652. DOI: 10.1515/HF.2006.109

Hubbe, M. A., and Bowden, C. (2009). "Handmade paper: A review of its history, craft, and science," *BioResources* 4(4), 1736-1792.

Hunter, D. (1978). *Papermaking: The History and Technique of an Ancient Craft*, Dover Publications, New York.

Isogai, A., and Berglund, L. A. (2013). "Preparation and applications of nanofibrillar celluloses," in: *Advances in Pulp and Paper Research*, *The 15th Pulp and Paper Fundamental Research Symposium* Cambridge, UK, 737-764.

Kars, G., and Gunduz, U. (2010). "Towards a super H_2 producer: Improvements in photofermentative biohydrogen production by genetic manipulations," *International Journal of Hydrogen Energy* 35, 6646-6656. DOI: 10.1016/j.ijhydene.2010.04.037

Lavoine, N., Desloges, I., Dufresne, A., and Bras, J. (2012). "Microfibrillated cellulose - Its barrier properties and applications in cellulosic materials: A review," *Carbohydrate Polymers* 90(2), 735-764. DOI: 10.1016/j.carbpol.2012.05.026

Liu, Y., Rafailovich, M. H., Malal, R., Cohn, D., and Chidambaram, D. (2009). "Engineering of bio-hybrid materials by electrospinning polymer-microbe fibers," *Proceedings of the National Academy of Sciences of the United States of America* 106 (34), 14201-14206. DOI: 10.1073/pnas.0903238106

Ma, C., Wang, X., Guo, L., Wu, X., and Yang, H. (2012). "Enhanced photo-fermentative hydrogen production by *Rhodobacter capsulatus* with pigment content manipulation," *Bioresource Technology* 118, 490-495. DOI: 10.1016/j.biortech.2012.04.105

McKinlay, J. B., Oda, Y., Rühl, M., Posto, A. L., Sauer, U., and Harwood, C. S. (2014). "Non-growing *Rhodopseudomonas palustris* increases the hydrogen gas yield from acetate by shifting from the glyoxylate shunt to the tricarboxylic acid cycle," *Journal of Biological Chemistry* 289(4), 1960-1970. DOI: 10.1074/jbc.M113.527515

Muzziotti, D., Adessi, A., Faraloni, C., Torzillo, G., and De Philippis, R. (2016). "H$_2$ Production in *Rhodopseudomonas palustris* as a way to cope with high light intensities," *Research in Microbiology* 167(5), 350-356.

Oh, Y. K., Seol, E. H., Kim, M. S., and Park, S. (2004). "Photoproduction of hydrogen from acetate by a chemoheterotrophic bacterium *Rhodopseudomonas palustris* P4," *International Journal of Hydrogen Energy* 29(11), 1115-1121. DOI: 10.1016/j.ijhydene.2003.11.008

Pirttijarvi, T. S. M., Andersson, M. A., and Salkinoja-Salonen, M. S. (2000). "Properties of *Bacillus cereus* and other bacilli contaminating biomaterial-based industrial processes," *International Journal of Food Microbiology* 60(2-3), 231-239. DOI: 10.1016/S0168-1605(00)00313-5

Priha, O., Hallamaa, K., Saarela, M., and Raaska, L. (2004). "Detection of *Bacillus cereus* group bacteria from cardboard and paper with real-time PCR," *Journal of Industrial Microbiology & Biotechnology* 31(4), 161-169. DOI: 10.1007/s10295-004-0125-x

Rey, F. E., Heiniger, E. K., and Harwood, C. S. (2007). "Redirection of metabolism for biological hydrogen production," *Applied and Environmental Microbiology* 73(5), 1665-1671. DOI: 10.1128/AEM.02565-06

Rey, F. E., Oda, Y., and Harwood, C. S. (2006). "Regulation of uptake hydrogenase and effects of hydrogen utilization on gene expression in *Rhodopseudomonas palustris*," *Journal of Bacteriology* 188(17), 6143-6152. DOI: 10.1128/JB.00381-06

Siqueira, G., Bras, J., and Dufresne, A. (2010). "Cellulosic bionanocomposites: A review of preparation, properties, and applications," *Polymers* 2(4), 728-765. DOI: 10.3390/polym2040728

Siro, I., and Plackett, D. (2010). "Microfibrillated cellulose and new nanocomposite materials: A review," *Cellulose* 17(3), 459-494. doi:DOI: 10.1007/s10570-010-9405-y

Show, K. Y., Lee, D. J., Tay, J. H., Lin, C. Y., and Chang, J. S. (2012). "Biohydrogen production: Current perspectives and the way forward," *International Journal of Hydrogen Energy* 37, 15616-15631. DOI: 10.1016/j.ijhydene.2012.04.109.

Stenstad, P., Andresen, M., Tanem, B. S., and Stenius, P. (2008). "Chemical surface modifications of microfibrillated cellulose," *Cellulose* 15(1), 35-45. DOI: 10.1007/s10570-007-9143-y

Suihko, M. L., and Skytta, E. (1997). "A study of the microflora of some recycled fibre pulps, boards, and kitchen rolls," *Journal of Applied Microbiology* 83(2), 199-207. DOI: 10.1046/j.1365-2672.1997.00219.x

Suihko, M. L., and Stackebrandt, E. (2003). "Identification of aerobic mesophilic bacilli isolated from board and paper products containing recycled fibres," *Journal of Applied Microbiology* 94(1), 25-34. DOI: 10.1046/j.1365-2672.2003.01803.x

Suominen, I., Suihko, M. L., and Salkinoja-Salonen, M. (1997). "Microscopic study of migration of microbes in food-packaging paper and board," *Journal of Industrial Microbiology & Biotechnology* 19(2), 104-113. DOI: 10.1038/sj.jim.2900424

TAPPI T-205 sp-95 (1995). "Forming handsheets for physical tests of pulp," TAPPI Press, Atlanta, GA.

Vaisanen, O. M., Mentu, J., and Salkinojasalonen, M. S. (1991). "Bacteria in food-packaging paper and board," *Journal of Applied Bacteriology* 71(2), 130-133.

Vaisanen, O. M., Nurmiaholassila, E. L., Marmo, S. A., and Salkinoja-Salonen, M. S. (1994). "Structure and composition of biological slimes on paper and board machines," *Applied and Environmental Microbiology* 60(2), 641-653.

Vaisanen, O. M., Weber, A., Bennasar, A., Rainey, F. A., Busse, H. J., and Salkinoja-Salonen, M. S. (1998). "Microbial communities of printing paper machines," *Journal of Applied Microbiology* 84(6), 1069-1084.

Zhang, Y., Nipelo, T., Salas, C., Arboleda, J., Hoeger, I., and Rojas, O. (2013). "Cellulose nanofibrils: From strong materials to bioactive surfaces," *Journal of Renewable Materials* 1(3), 195-211.

Zimmermann, T., Pohler, E., and Geiger, T. (2004). "Cellulose fibrils for polymer reinforcement," *Advanced Engineering Materials* 6(9), 754-761. DOI: 10.1002/adem.200400097